~~CONFIDENTIAL~~

Copy
RM L57C17

NACA RM L57C17

NACA

RESEARCH MEMORANDUM

TRANSONIC WIND-TUNNEL INVESTIGATION OF STATIC-PRESSURE FLUCTUATIONS IN DUCT OF A SCALE INLET MODEL OF A SUPERSONIC FIGHTER-BOMBER AIRPLANE

By Joseph D. Brooks

Langley Aeronautical Laboratory
Langley Field, Va.

NATIONAL ADVISORY COMMITTEE
FOR AERONAUTICS

WASHINGTON
August 6, 1957

~~CONFIDENTIAL~~

NACA RM L57C17

NATIONAL ADVISORY COMMITTEE FOR AERONAUTICS

RESEARCH MEMORANDUM

TRANSONIC WIND-TUNNEL INVESTIGATION OF STATIC-PRESSURE FLUCTUATIONS IN DUCT OF A SCALE INLET MODEL OF A SUPERSONIC FIGHTER-BOMBER AIRPLANE

By Joseph D. Brooks

SUMMARY

A transonic investigation of the static-pressure fluctuations in the left duct of a scale inlet model of a supersonic fighter-bomber airplane has been conducted in the Langley 8-foot transonic tunnel. The model consisted of the forward part of the fuselage with wing stubs incorporating wing leading-edge scoop-type inlets. The amplitude and frequency of the pressure fluctuations were measured by means of an electrical pressure gage mounted flush with the diffuser wall at Mach numbers of 0.90, 0.95, and 1.10 at mass-flow ratios that varied from approximately 0.60 to the maximum obtainable. Measurements were made at angles of attack from -4° to 10° and angles of yaw from -10° to 5.2°.

The maximum pressure fluctuations were comparatively low and did not exceed 4 percent of free-stream total pressure. The largest fluctuations occurred at the maximum mass-flow ratio at each Mach number. A decrease in the height of the boundary-layer diverter at Mach numbers of 0.90 and 1.10 reduced appreciably the effect of yaw on the pressure fluctuations at the high mass-flow ratios. Power-spectral analyses of these data indicate considerable power in the spectra at the predominant duct resonant frequency at each Mach number. An increase in the flow distortions at the compressor face is generally associated with an increase in the amplitude of the pressure fluctuations.

INTRODUCTION

A transonic investigation of the aerodynamic characteristics of a scale inlet model of a supersonic fighter-bomber airplane with wing leading-edge scoop-type inlets was made in the Langley 8-foot transonic tunnel. The investigation provided information on the pressure recovery, the flow distortion in the duct at the station corresponding to the

engine face, and the pressure fluctuations in the diffuser section of the left duct. The purpose of this paper is to show the amplitude and frequencies of the pressure fluctuations at transonic speeds. Large pressure fluctuations at a particular frequency can be very destructive to the ducting and to the aircraft engine and, in addition, the performance of a diffuser is reduced by instability. It is difficult to predict the stability of any particular configuration, and little information is available on pressure fluctuations in supersonic inlets at transonic speeds.

The pressure fluctuations were measured at Mach numbers of 0.90, 0.95, and 1.10 at mass-flow ratios that varied from approximately 0.60 to the maximum obtainable. Measurements were made at angles of yaw from -10° to approximately 5° and a few measurements were made at angles of attack up to 10°. At the higher mass-flow ratios at Mach numbers of 0.90 and 1.10, measurements were also obtained with gloves on the body that reduced the height of the boundary-layer diverter at each inlet.

SYMBOLS

A	duct cross-sectional area
A_p	projected area of inlet (5.00 sq in. on model)
C_p	pressure coefficient, $\frac{p - p_\infty}{q}$
p	local static pressure
p_t'	local total pressure
$\frac{p_t'}{(p_t')_\infty}$	duct local total-pressure ratio
M	free-stream Mach number
q	free-stream dynamic pressure, $\frac{1}{2}\rho_\infty V_\infty^2$
V	velocity of flow in duct
w	duct mass-flow rate, ρAV

[redacted]

w/w_∞ duct mass-flow ratio; value based on projected area of inlet, $\frac{w}{\rho_\infty V_\infty A_p}$

α angle of attack of model measured from fuselage horizontal center line, deg

Δp pressure fluctuation across diaphragm of electrical pressure gage

$\left(\frac{\Delta p}{q}\right)_{max}$ maximum pressure-fluctuation coefficient of Δp (peak to peak)

$\left(\frac{\Delta p}{q}\right)_{rms}$ root-mean-square pressure-fluctuation coefficient of Δp

$\frac{(\Delta p/q)^2}{cps}$ power-spectral-density function of Δp

ρ mass density of flow in duct

ψ angle of yaw of model, measured positive when model nose is to the right, deg

Subscript:

∞ free stream

APPARATUS AND TESTS

Tunnel

The fluctuating pressure measurements reported herein were made in the duct of an inlet model in the Langley 8-foot transonic tunnel. This tunnel has a slotted test section to allow continuous operation through the transonic speed range and operates at a stagnation pressure approximately equal to atmospheric pressure. During this investigation the tunnel stagnation temperature varied, depending on atmospheric conditions, from approximately 115° F to 130° F at M = 0.90, 125° F to 145° F at M = 0.95, and 140° F to 160° F at M = 1.10. A detailed description and calibration of the tunnel are presented in reference 1.

Model

The model used in this investigation is a scale inlet model of a supersonic fighter-bomber airplane. The model included the forward part

of the airplane fuselage with wing stubs incorporating wing leading-edge scoop-type inlets. Measurements were obtained with and without a glove attached to each side of the fuselage. The gloves widened the fuselage and in effect reduced the height of the boundary-layer diverter. A sketch of the model is shown in figure 1 and photographs of the model are shown in figures 2 and 3.

Each semielliptical duct from the left and right inlets converges and forms a semicircular duct as shown in the section drawings of figure 1. The divider plate that separates the semicircular ducts terminates behind the station corresponding to the engine face location. A motor-driven throttle at the base of the model was used during the investigation for varying the mass flow in the model. Figure 4 shows the variation of the total duct cross-sectional area with fuselage station.

Instrumentation

The pressure fluctuations were measured at the lower surface of the left duct with an electrical pressure gage of the type described in reference 2. The gage was located approximately midway between the inlet and the station corresponding to the engine face as indicated in figure 1. The pressure gage was referenced to a steady pressure and the electrical signal from the gage was amplified and recorded by an oscillograph and a tape recorder. A part of two typical oscillograph records is shown in figure 5.

Mass flow through the duct system was computed from the average of the values determined from two survey rakes - an upstream rake located at the fuselage station corresponding to the engine face and a downstream rake located near the exit of the duct. The rake located at the station corresponding to the engine face was also used for pressure profile studies and contained 28 total-pressure tubes and 9 static-pressure tubes.

The angle of attack was measured by a strain-gage attitude transmitter. The instrument was mounted in the fuselage.

Tests

Data were obtained at mass-flow ratios that varied from approximately 0.60 to the maximum obtainable at Mach numbers of 0.90, 0.95, and 1.10. Measurements were made at angles of attack from -4° to 10° generally at reduced mass-flow ratios and at angles of yaw from -10° to 5.2° at mass-flow ratios above 0.80. At Mach numbers of 0.90 and 1.10, measurements were also made with gloves on the fuselage and with a transition strip 5.5 inches from the model nose. The free-stream

Reynolds number based on a length of 1 foot varied from 3.8×10^6 to 4.1×10^6.

Reduction of Data and Accuracy

For each test point, a power-spectral analysis and an overall root-mean-square pressure was obtained from the tape recordings with an electronic analog analyzer. The tape-recording system and the electronic analyzer are described in reference 3. The maximum peak-to-peak pressure fluctuations were determined from the oscillograph records as shown in figure 5.

Because of the random nature of the flow, each test point of the data was obtained over a period of 45 seconds, and 15-second data samples were analyzed.

The accuracy of the root-mean-square and the maximum pressure-fluctuation coefficients are estimated to be within ±10 percent in the frequency range from 0 to 700 cps. The power spectra have a frequency range from about 25 to 700 cps and the frequency scales on the figures are estimated to be correct within ±15 cps. The amplitudes of the power spectra are believed to be correct within ±10 percent except for the high amplitude peaks (at resonant frequencies) that are much larger and narrower than indicated. No attempt was made to correct these peaks since the relative amplitudes shown in the figures are comparable.

The average stream Mach number was held within ±0.003 of the nominal value given in the figures. The model angle of attack and angle of yaw are estimated to be correct within $\pm 0.1^\circ$.

RESULTS AND DISCUSSION

Amplitude Characteristics of Pressure Fluctuations

The variation of the root-mean-square pressure coefficient and the maximum pressure coefficient with mass-flow ratio for various angles of attack and yaw are shown in figure 6. Flags on the symbols serve to identify the test points with transition strip and those with gloves on the fuselage. The root-mean-square turbulence level in the tunnel, measured in the vertical plane of the free-stream flow with a 3° conical probe, is included in the figure.

The overall variation of the root-mean-square pressure-fluctuation coefficients with mass-flow ratio in figure 6 is approximately the same as the variation of the maximum values at each Mach number.

[redacted]

With increasing mass-flow ratio up to 0.80, only a small variation in the pressure fluctuations occurs at each Mach number. The level of the fluctuations is low and some of the root-mean-square values are only about 30 percent larger than the level of the tunnel turbulence. At mass-flow ratios above 0.80, the pressure fluctuations increased very rapidly. The largest fluctuations occurred at the maximum obtainable mass-flow ratio at each Mach number and are approximately three to five times those measured at mass-flow ratios below 0.80. Unpublished data indicate that the inlet is choked at the maximum obtainable mass-flow ratio.

The amplitude of the pressure fluctuations generally increases as the angle of yaw increases at mass-flow ratios above 0.80 (fig. 6). The largest values measured are at $\psi = -10^{\circ}$ when the left inlet, containing the electrical pressure gage, is blanketed or shielded by the forward part of the body. (No data were obtained at $\psi = 10^{\circ}$.) The steady-state pressure coefficients on the left side of the fuselage, forward of the left inlet, are shown in figure 7 at various angles of yaw at Mach numbers of 0.90 and 1.10. In figure 7, the pressure coefficients become positive at the inlet (21 inches from the model nose) and there is no indication of flow separation at least from the nose of the model back to the inlet.

The effects of the fuselage gloves on the pressure fluctuations at various angles of yaw are shown in figure 6 at mass-flow ratios of approximately 0.83 and 0.87 and at Mach numbers of 0.90 and 1.10. With gloves on the fuselage, the pressure fluctuations do not vary appreciably at either Mach number or mass-flow ratio when the model is yawed. At a mass-flow ratio of 0.83, the fluctuations with gloves on the model are reduced to about the same amplitude as those measured at reduced mass-flow ratios without gloves. Comparing the effect of the fuselage gloves on the pressure coefficients at a yaw angle of -10° (fig. 7) indicates that the fuselage gloves reduce the adverse pressure gradient forward of the inlet.

No appreciable effect of the fuselage transition strip and angle of attack was noted in figure 6. A few measurements at large angles of attack or at combined angles of attack and yaw indicate an increase in the amplitude of the fluctuations; however, a complete range of measurements was not obtained, particularly at high mass-flow ratios.

In reference 4, the results of an investigation of the air-flow stability in the duct of an airplane model with scoop-type normal-shock inlets are presented at 0° angle of attack and yaw. The magnitude of the maximum (peak-to-peak) pressure fluctuations varied from 1 to 2 percent of free-stream total pressure at Mach numbers of 0.80 and 1.30, respectively. The magnitude of the largest fluctuations obtained in the present investigation, without gloves on the fuselage, vary from

approximately 3 percent of free-stream total pressure at a Mach number of 0.90 to about 4 percent at a Mach number of 1.10. With gloves on the fuselage, the fluctuations were reduced to about 2 percent at a Mach number of 0.90 and 3 percent at a Mach number of 1.10. It appears that the maximum pressure fluctuations that occurred in this investigation are comparatively low considering the complex ducting system employed in the model.

Power-Spectral Analyses

Power spectra of the pressure fluctuations are shown in figures 8, 9, and 10. When possible, comparisons are made to show the general effect of Mach number, mass-flow ratio, angle of yaw with and without gloves, and angle of attack. Each point on these spectra represents an estimate of the average power of a frequency band width of about 25 cps. This band width results in a reduction in the amplitude and sharpness to peaks narrower than 25 cps. Because of this, analyses were made of a few test points, obtained at reduced mass-flow ratios, using a filter band width of 3 cps. The resulting spectra indicated a large peak, or spike, at a frequency of about 400 cps at Mach numbers of 0.90 and 0.95 and at about 250 cps at a Mach number of 1.10. The true amplitude of the spectrum at the spike can be estimated by considering all of the power in the peak shown in the figures concentrated at the peak frequency.

A theoretical calculation of the fundamental duct resonant frequency was made for the supersonic Mach number of 1.10 at a mass-flow ratio of 0.70 by using the quasi-one-dimensional-flow (plane-wave) theory of reference 5. The time required for a wave to travel from the inlet to the exit and then return to the inlet resulted in a frequency of approximately 236 cps. This is in fair agreement with the peak that appears in the spectra at a Mach number of 1.10.

According to the data presented in reference 5, it appears that the frequency measured in the model duct can be scaled to the full-scale airplane for the same test conditions by the inverse ratio of the duct lengths. It is believed that the amplitude of the fluctuations measured in the model would be nearly equal to that measured in the full-scale airplane for a given duct location.

Power spectra of the pressure fluctuations in free-stream flow and in the model duct, at $\alpha = 0^\circ$ and $\psi = 0^\circ$, at a moderate and a high mass-flow ratio are shown in figures 8(a) and 8(b) at Mach numbers of 0.90 and approximately 1.10, respectively. At the moderate mass-flow ratio, the root-mean-square pressure fluctuation coefficients measured in the model duct are not appreciably larger than those measured in the free-stream flow in the tunnel, but no peak appears in the spectrum of the free-stream flow at the duct resonant frequencies at either Mach

number in figure 8. When the mass-flow ratio is increased to the maximum obtainable, most of the increase in power, at $\alpha = 0^\circ$ and $\psi = 0^\circ$, occurs in the lower frequency range up to 350 cps. No effect of Mach number is noted other than the difference in the predominant duct resonant frequencies.

The effect of yaw on the spectra of the fluctuations is shown for each test Mach number at $\alpha = 0^\circ$ and at mass-flow ratios of approximately 0.83 and 0.87 in figures 9(a) and 9(b), respectively. (A logarithmic scale is used for the ordinate in these figures.) A change in angle of yaw from 0° to 5° or -10° without gloves on the fuselage generally resulted in an increase in power over the frequency range from about 100 cps to 700 cps, with the greatest increase occurring at a yaw angle of -10°. At Mach numbers of 0.90 and 1.10, the spectra obtained with the gloves on the fuselage are also shown in figures 9(a) and 9(b), respectively. With gloves on, there is no appreciable effect of yaw on the spectra of the pressure fluctuations at either Mach number or mass-flow ratio. At the subsonic Mach numbers, the peaks at the fundamental resonant frequency and at harmonics are small; however, at the supersonic Mach number of 1.10 large peaks sometimes appear in the spectra at frequencies of approximately 250 cps and also at 500 cps.

At a mass-flow ratio of approximately 0.52 and a Mach number of 0.90, fluctuation measurements were made at various angles of attack and an angle of yaw of 0°. The spectra from these measurements are shown in figure 10(a). Decreasing the angle of attack to -4° had no appreciable effect on the spectra; however, when the angle of attack is increased to 10°, the resonant peak at 400 cps doubled in amplitude. In figure 10(b) the spectrum at $\alpha = 10^\circ$ and $\psi = 5.2^\circ$ is compared with the spectrum at $\alpha = 0^\circ$ and $\psi = 0^\circ$ at a Mach number of 1.10 and a mass-flow ratio of about 0.7. The combined effect of angle of attack and yaw resulted in a general increase in power over the complete frequency range. The results obtained are not conclusive since a complete range of measurements was not made, as previously noted.

Flow Distortions at Compressor Face

In order to correlate the flow distortions at the compressor face with the fluctuating pressure measurements, contour maps of total-pressure ratio at the compressor face are shown in figures 11 and 12 at Mach numbers of 0.90 and 1.10, respectively. Comparison of contour maps with and without gloves on the fuselage is not shown, since no appreciable effect of gloves was noted in the values of total-pressure ratio at the compressor face.

At a moderate mass-flow ratio, the flow appears to be uniform at $\alpha = 0^\circ$ and $\psi = 0^\circ$ in figures 11(a) and 12(a). By comparing the contour maps at a moderate mass-flow ratio with those at the maximum obtainable mass-flow ratio shown in figures 11(c) and 12(c) at $\alpha = 0^\circ$ and $\psi = 0^\circ$, it appears that at the high mass-flow ratio the boundary layer has thickened appreciably on the outer walls of the duct, particularly near the top, resulting in large flow distortions. At a yaw angle of -10° (figs. 11(d) and 12(d)), the boundary layer has thickened primarily at the top of the left duct. At the higher mass-flow ratio shown in figure 11(d), the flow distortion is appreciable. At an angle of attack of 10° the flow is fairly uniform (fig. 11(b)); however, the boundary layer has thickened in the lower portion of both ducts. The combined effects of yaw and angle of attack (fig. 12(b)) have resulted in an unsymmetrical flow distortion in the left and right ducts. There appears to be no appreciable effect of Mach number on the flow distortions as shown by comparing figure 11 with figure 12.

In general, the increases in flow distortions at the compressor face for the larger angles of attack and yaw and at the maximum obtainable mass-flow ratio correspond with increases in the magnitude of the pressure fluctuations shown in figure 6.

CONCLUSIONS

An investigation of the static-pressure fluctuations in the left duct of a scale inlet model of a supersonic fighter-bomber airplane, made in the Langley 8-foot transonic tunnel, at angles of attack from -4° to 10° and angles of yaw from -10° to 5.2°, leads to the following conclusions:

1. The maximum (peak-to-peak) values of the pressure fluctuations were comparatively low and did not exceed 4 percent of free-stream total pressure.

2. No appreciable change with mass-flow ratio in the amplitude of the pressure fluctuations at mass-flow ratios below 0.80 was noted. At mass-flow ratios above 0.80, the amplitude of the pressure fluctuations increased as the mass-flow ratio increased with the largest fluctuations occurring at the maximum obtainable mass-flow ratio which corresponded with the onset of choke.

3. At mass-flow ratios above 0.80, the amplitude of the fluctuations increased with increasing angle of yaw. The gloves, that were placed on the sides of the fuselage at Mach numbers of 0.90 and 1.10 to reduce the height of the boundary-layer diverter, reduced appreciably the effect of yaw on the amplitude of the pressure fluctuations.

4. Power-spectral analyses of these data indicate considerable power in the spectra at the predominant duct resonant frequency at each Mach number. When the mass-flow ratio is increased to the maximum obtainable at $\alpha = 0^{\circ}$ and $\psi = 0^{\circ}$, the power increased primarily in the lower frequency range up to 350 cps.

5. No appreciable effect of Mach number was noted in the investigation other than the shift in the predominant resonant peak to lower frequencies with increasing Mach number.

6. An increase in the flow distortions at the compressor face is generally associated with an increase in the amplitude of the pressure fluctuations.

Langley Aeronautical Laboratory,
National Advisory Committee for Aeronautics,
Langley Field, Va., March 26, 1957.

REFERENCES

1. Ritchie, Virgil S., and Pearson, Albin O.: Calibration of the Slotted Test Section of the Langley 8-Foot Transonic Tunnel and Preliminary Experimental Investigation of Boundary-Reflected Disturbances. NACA RM L51K14, 1952.

2. Patterson, John L.: A Miniature Electrical Pressure Gage Utilizing a Stretched Flat Diaphragm. NACA TN 2659, 1952.

3. Smith, Francis B.: Analog Equipment for Processing Randomly Fluctuating Data. Aero. Eng. Rev., vol. 14, no. 5, May 1955, pp. 113-119.

4. Mossman, Emmet A., Lazzeroni, Frank A., and Pfyl, Frank A.: An Experimental Investigation of the Air-Flow Stability of a Scoop-Type Normal-Shock Inlet. NACA RM A55A13, 1955.

5. Trimpi, Robert L.: A Theory for Stability and Buzz Pulsation Amplitude in Ram Jets and an Experimental Investigation Including Scale Effects. NACA Rep. 1265, 1956. (Supersedes NACA RM L53G28.)

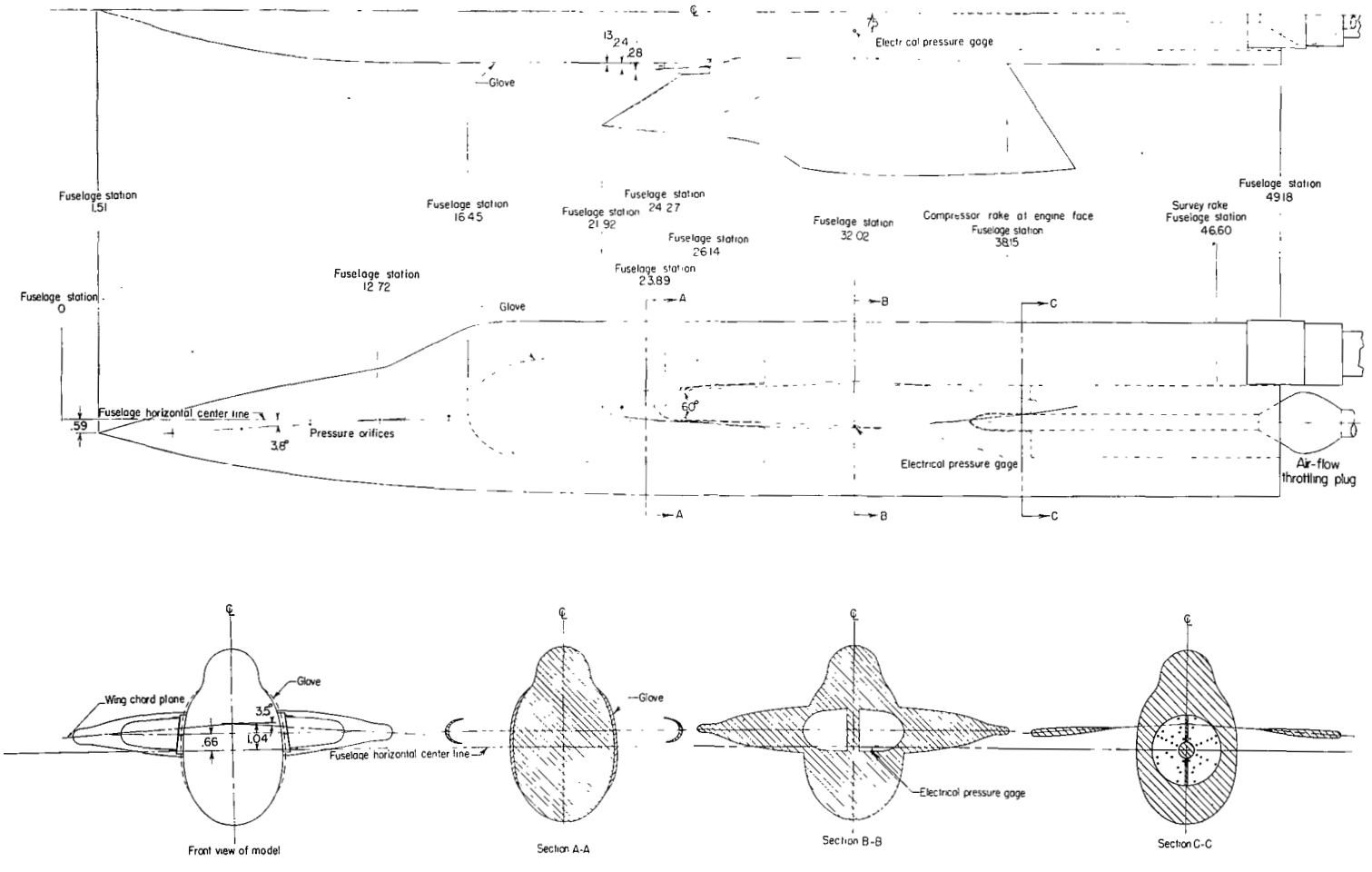

Figure 1.- Sketch of inlet model. All dimensions and fuselage stations are in inches.

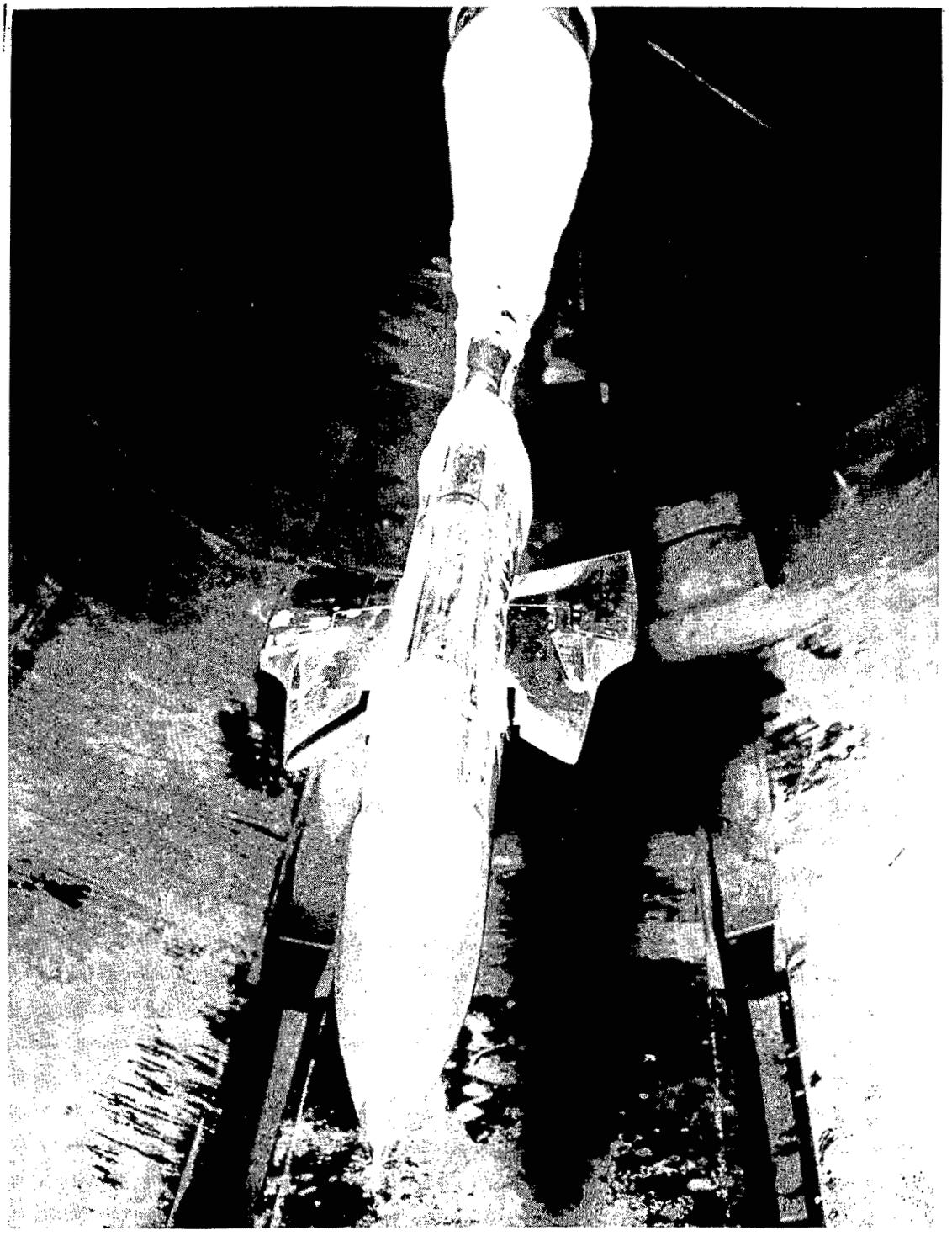

Figure 2.- Basic configuration showing transition strip on fuselage.

L-89261

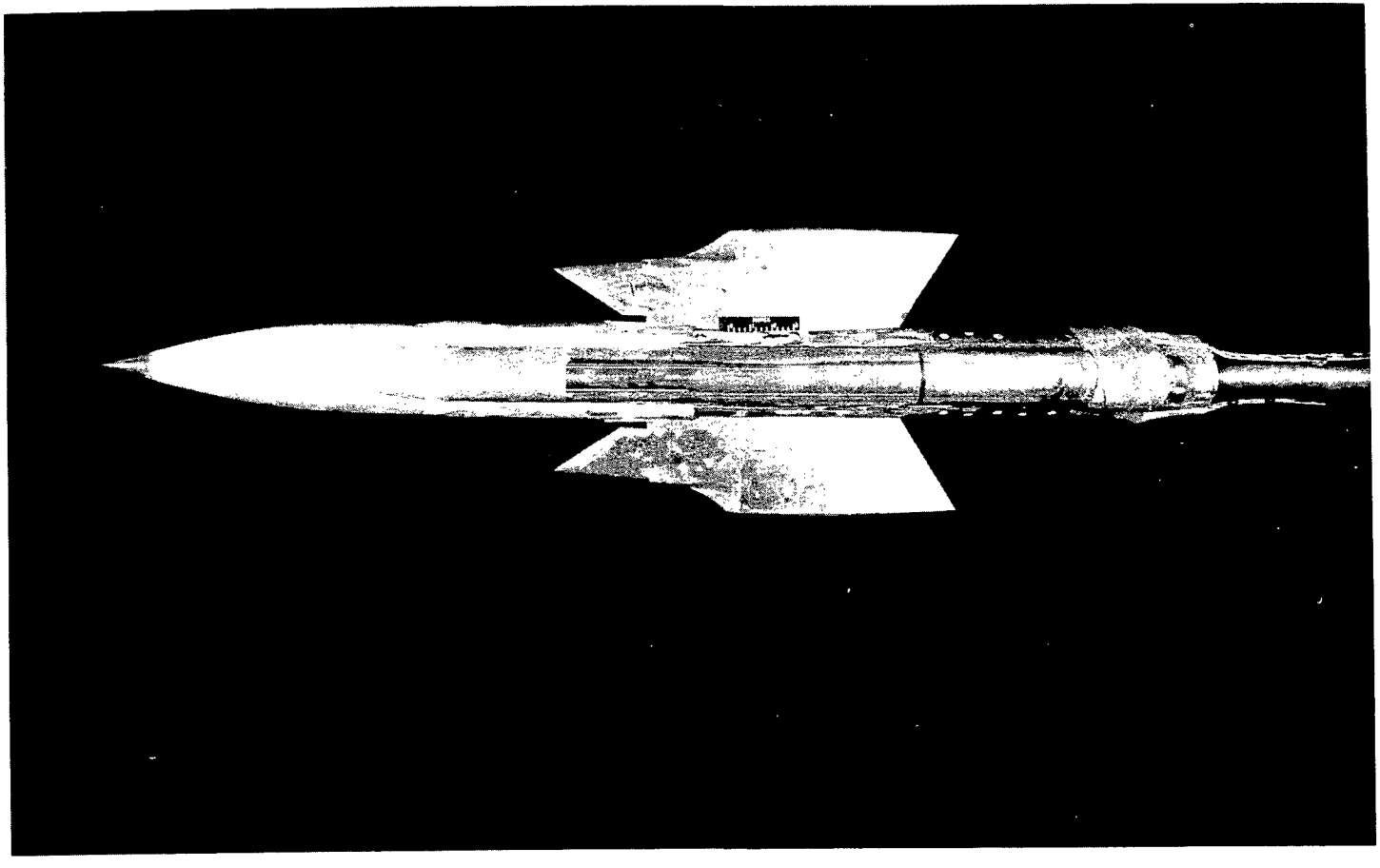

(a) Plan view. L-89411

Figure 3.- Basic configuration showing gloves on fuselage.

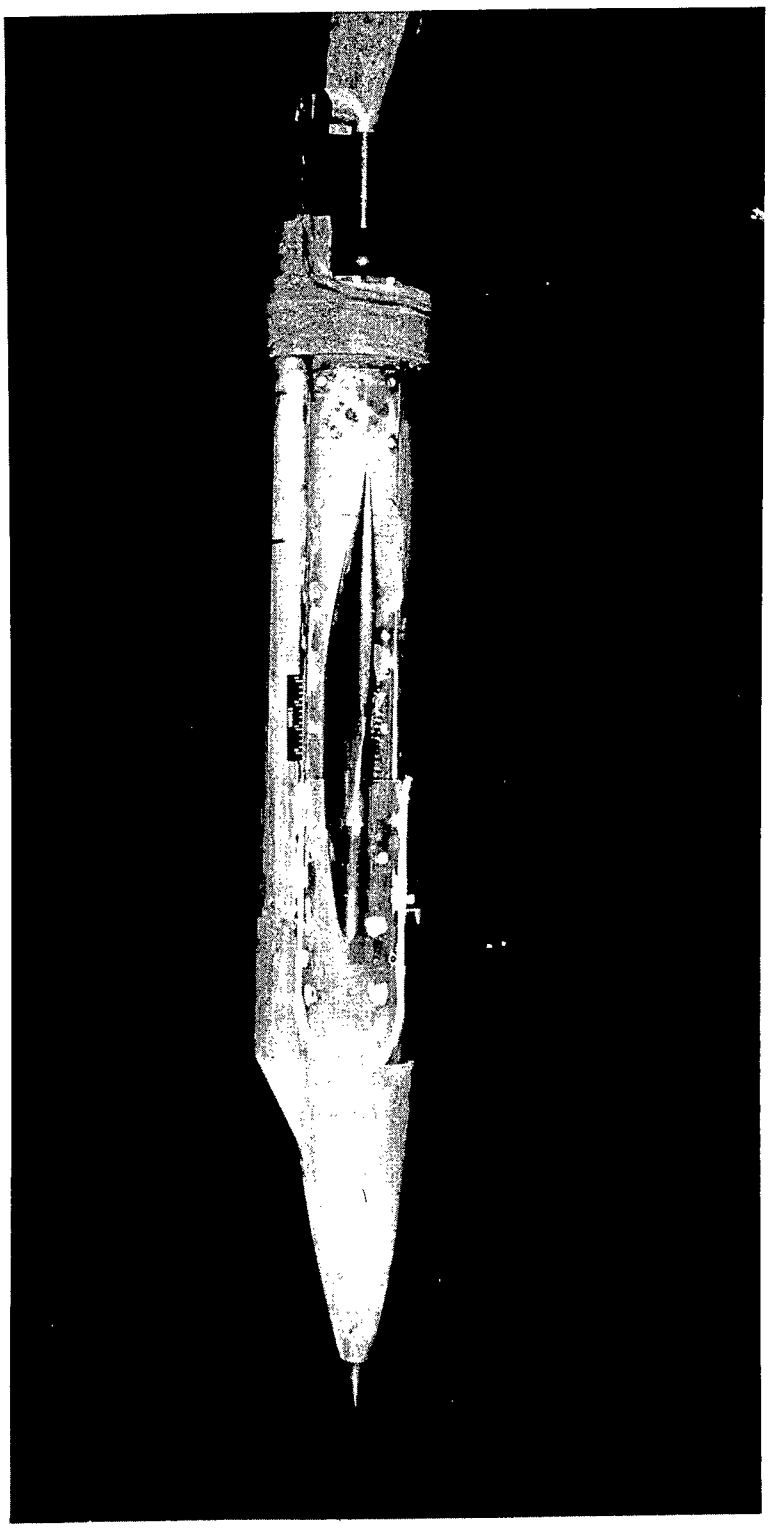

L-89410

(b) Side view.

Figure 3.- Concluded.

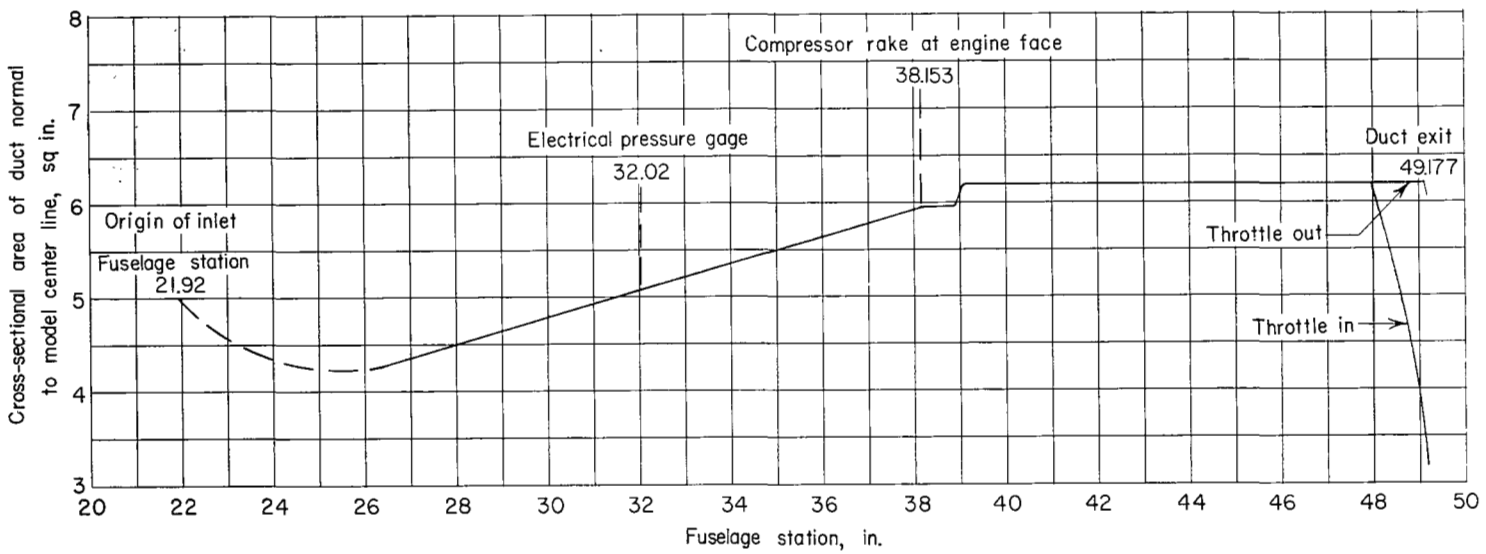

Figure 4.- Variation of total duct cross-sectional area with fuselage station.

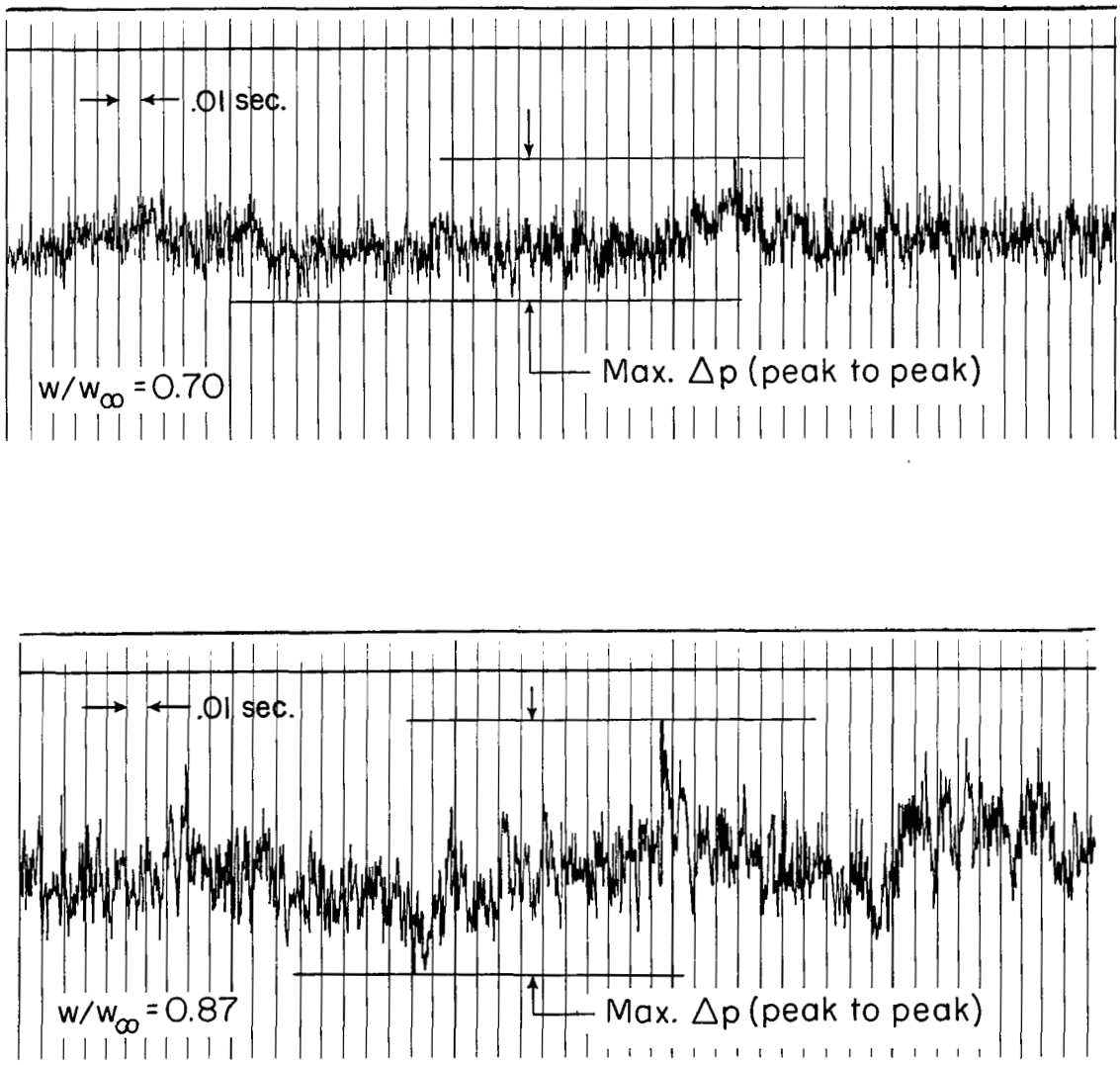

Figure 5.- Typical time histories of pressure fluctuations. M = 1.10.

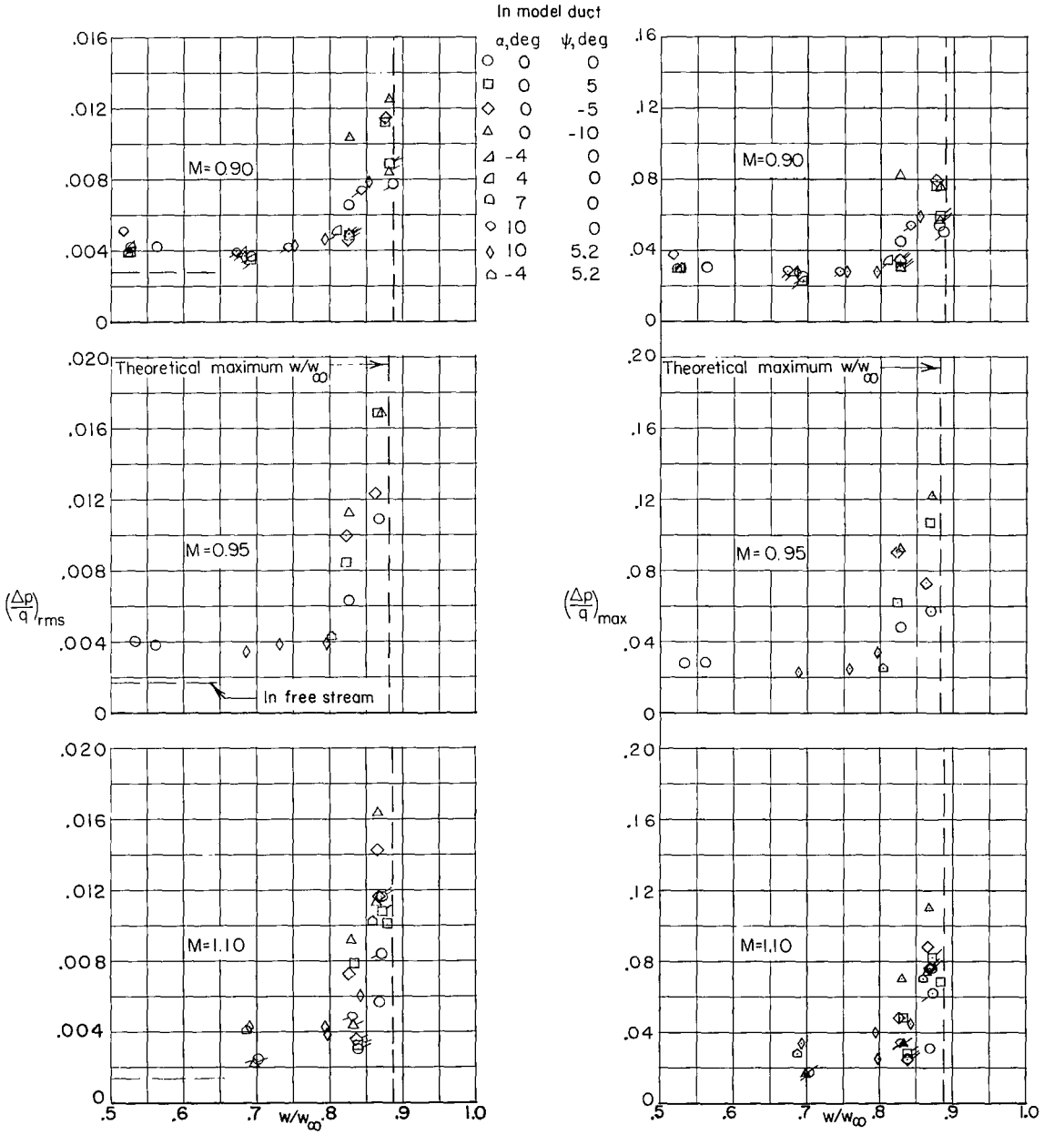

Figure 6.- Variation of root-mean-square and maximum pressure-fluctuation coefficients with mass-flow ratio. (Upper flags on symbols indicate gloves on fuselage, and lower flags on symbols indicate transition strip on fuselage.

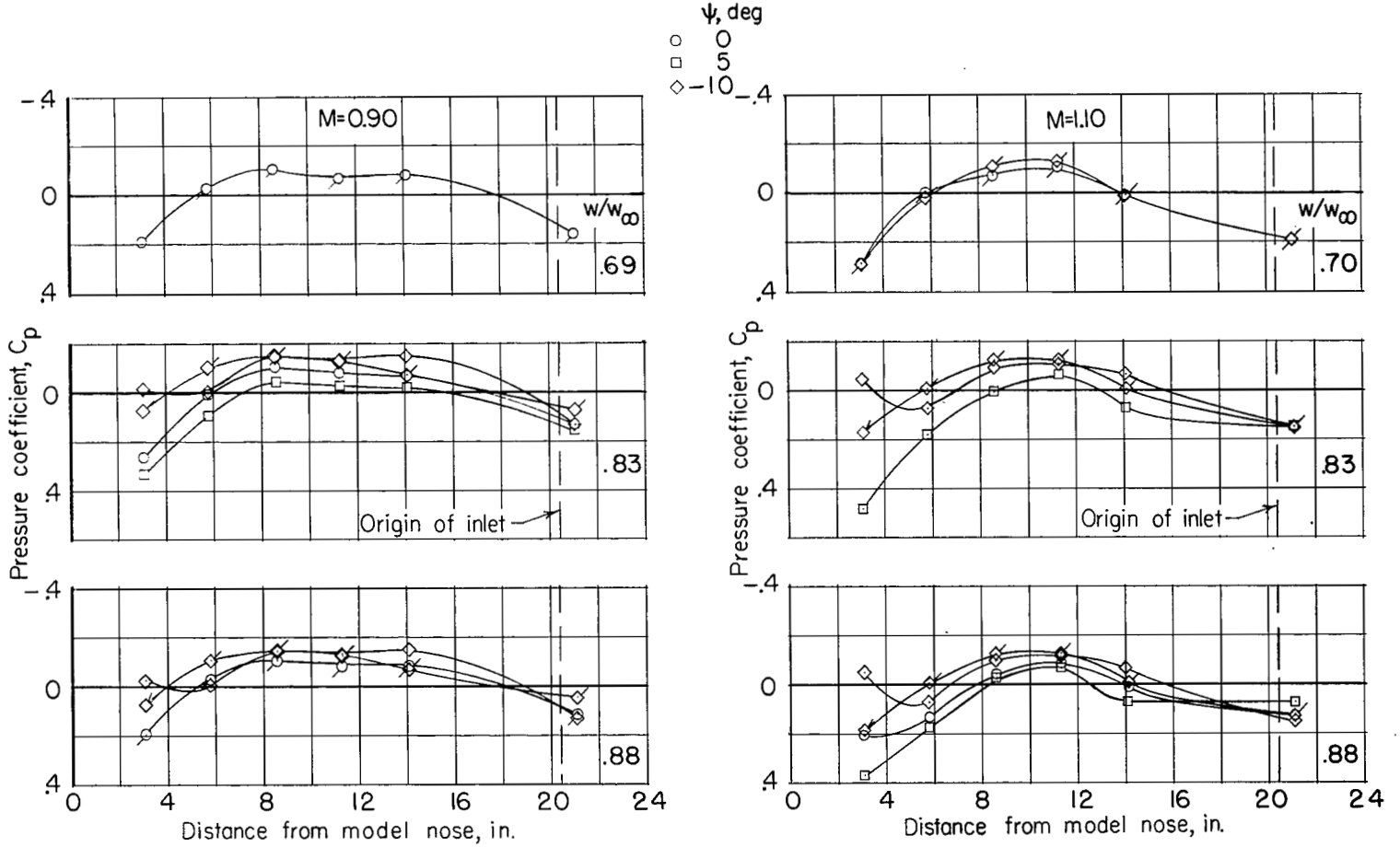

Figure 7.- Effect of ψ on the pressure coefficients on the left side of the fuselage forward of the inlet. Upper flags on symbols indicate gloves on fuselage and lower flags on symbols indicate transition strip on fuselage. $\alpha = 0^{\circ}$.

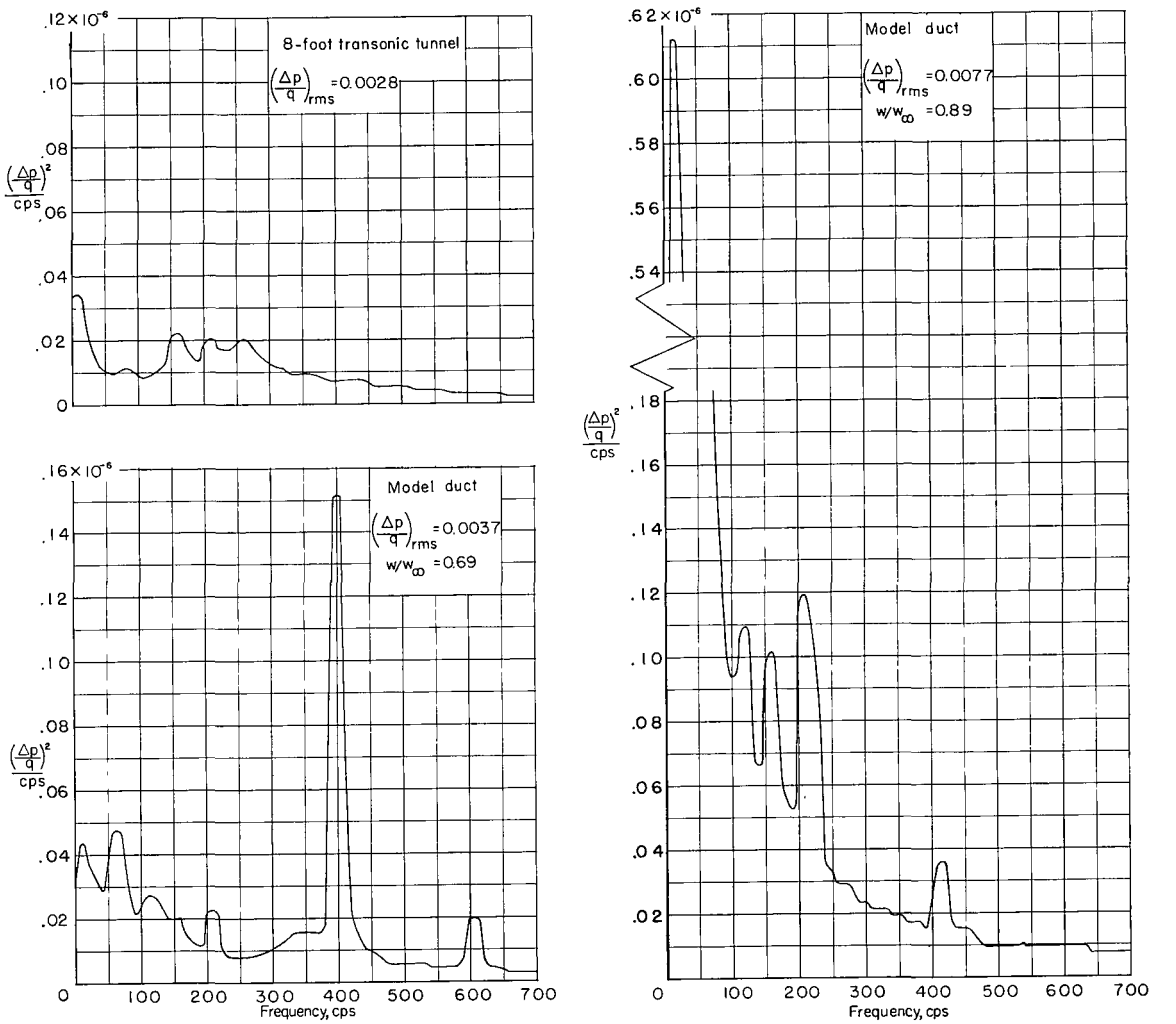

(a) M = 0.90.

Figure 8.- Power spectra of the pressure fluctuations in the tunnel and in the model duct at a moderate and a high mass-flow ratio. Transition strip on fuselage; $\alpha = 0^\circ$; $\psi = 0^\circ$.

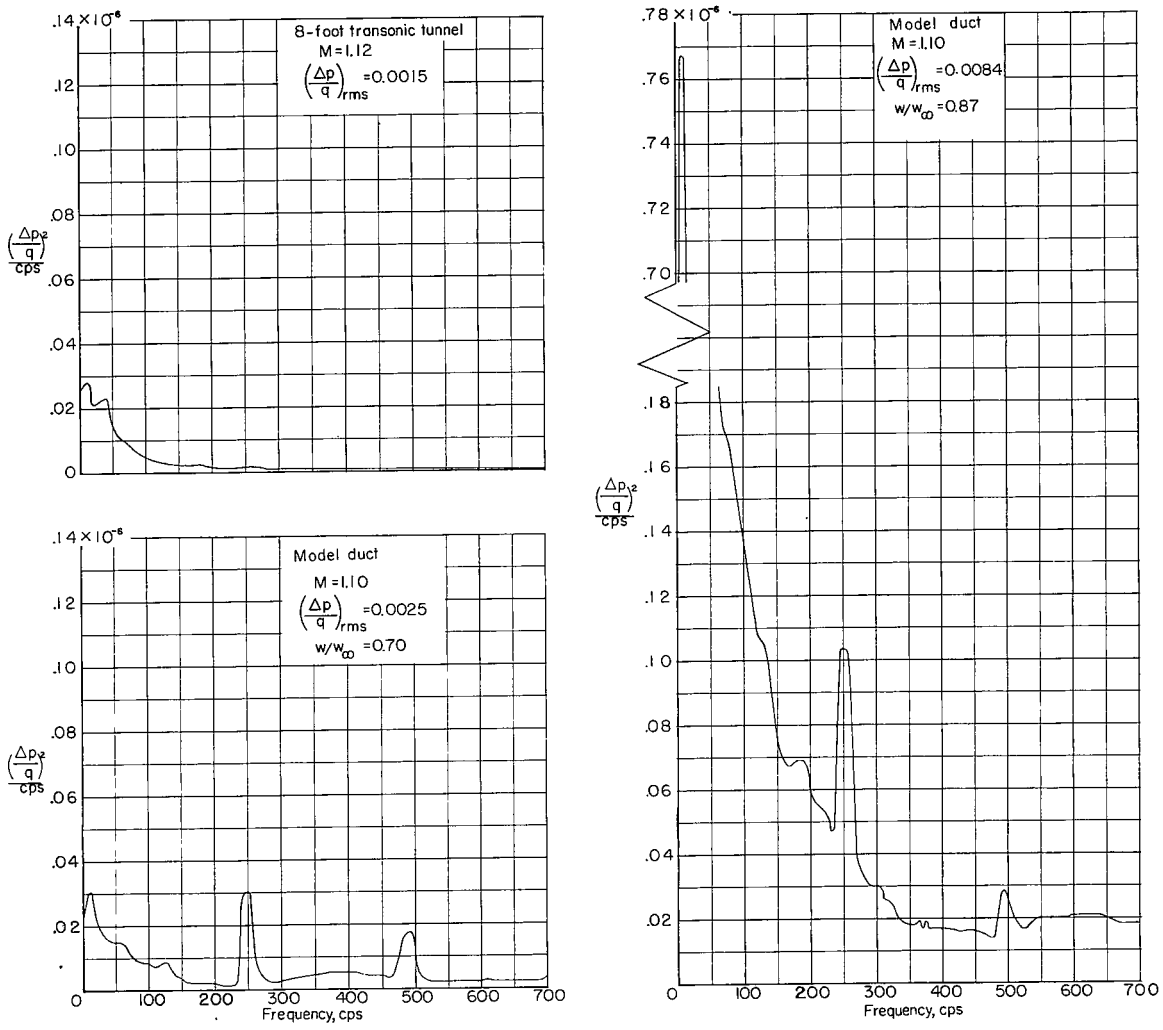

(b) $M \approx 1.10$.

Figure 8.- Concluded.

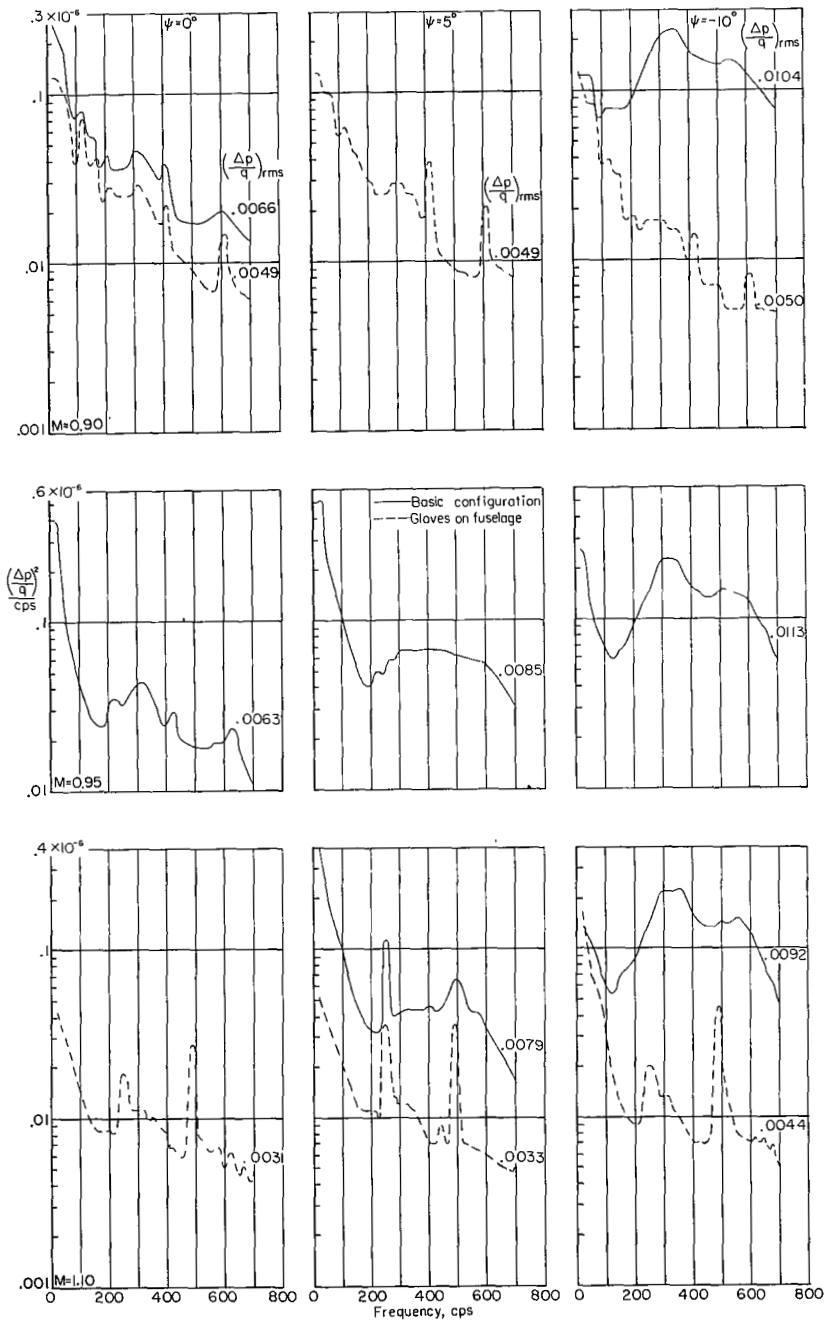

(a) $w/w_\infty \approx 0.83$.

Figure 9.- Effect of angle of yaw on the power spectra of the pressure fluctuations with and without gloves on the fuselage. $\alpha = 0^\circ$.

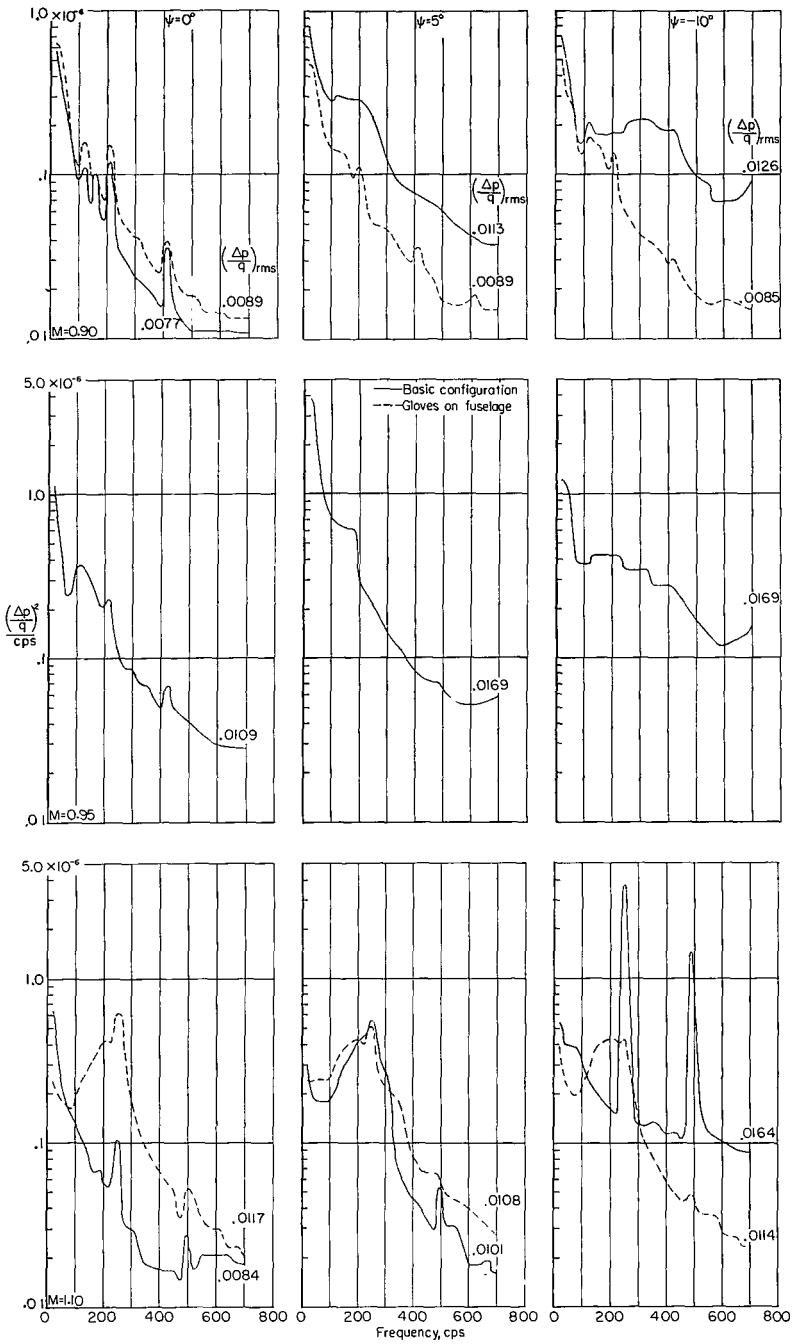

(b) $w/w_\infty \approx 0.87$.

Figure 9.- Concluded.

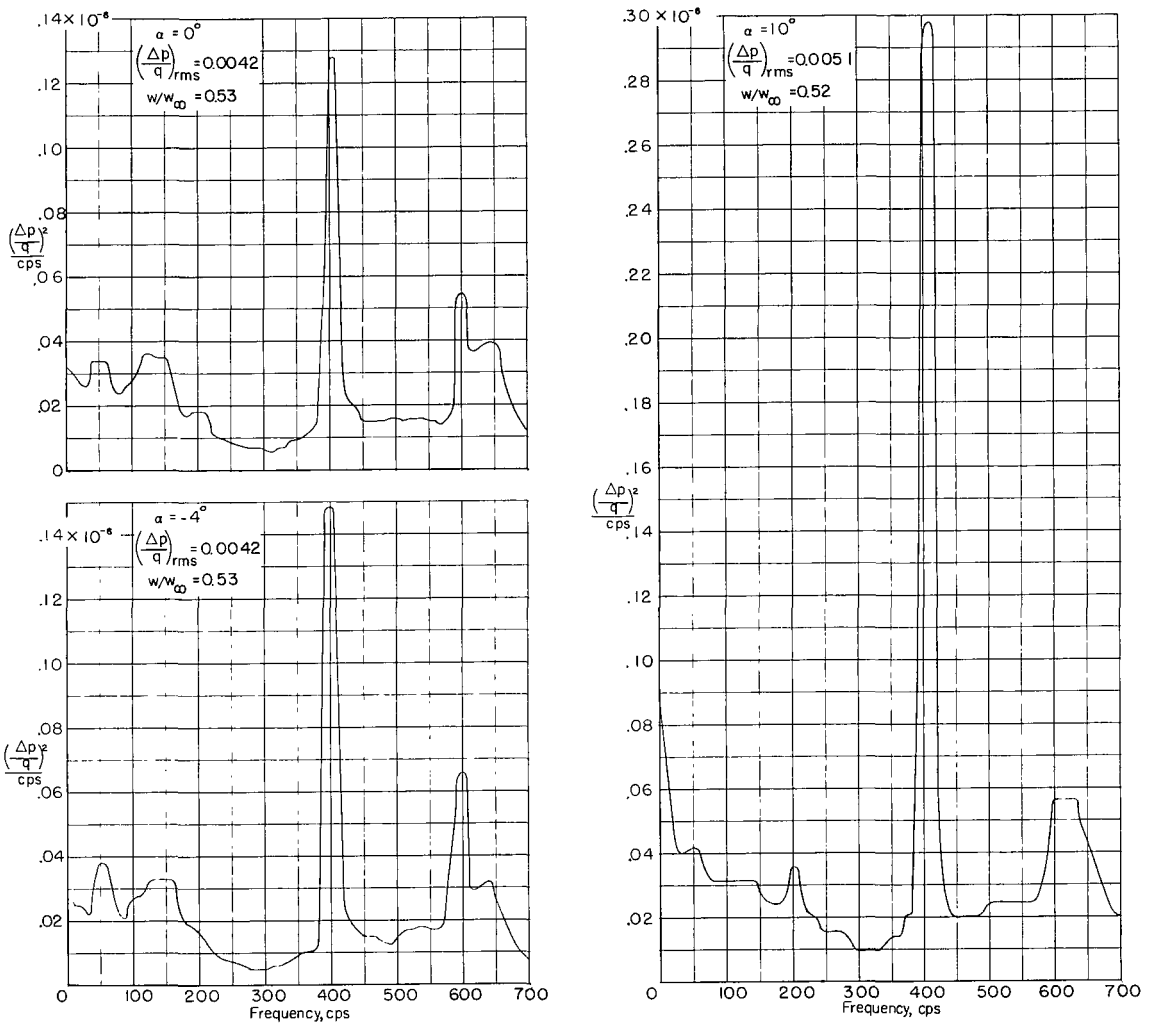

(a) M = 0.90; ψ = 0°.

Figure 10.- Effect of angle of attack on the power spectra of the pressure fluctuations.

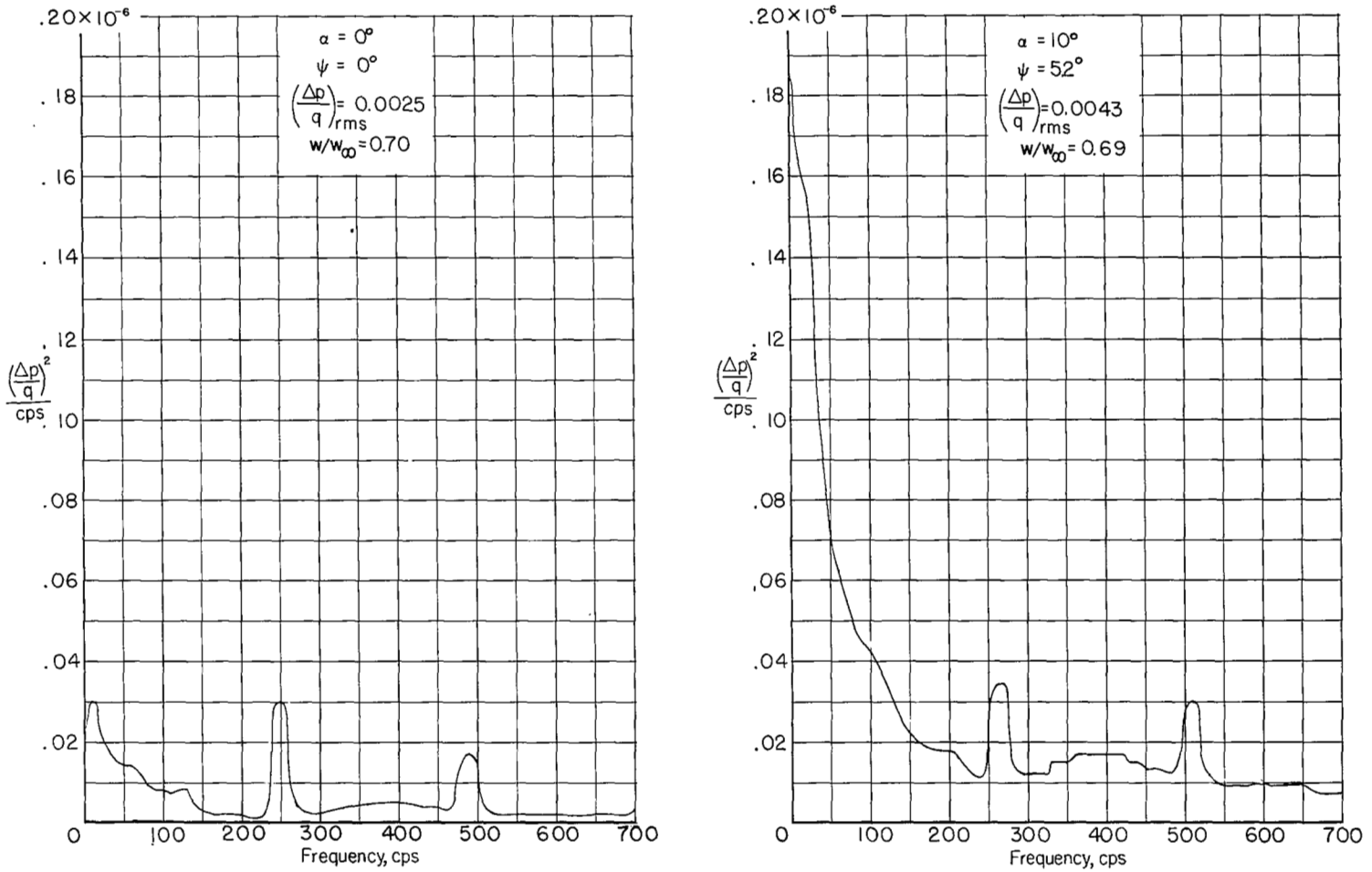

(b) M = 1.10.

Figure 10.- Concluded.

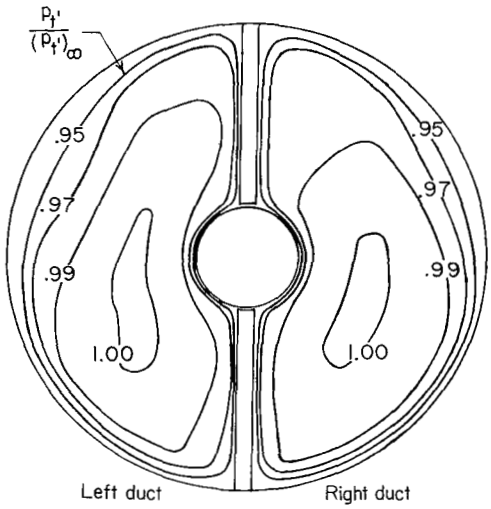

(a) $w/w_\infty = 0.53$; $\alpha = 0^\circ$; $\psi = 0^\circ$; average static-pressure ratio, 0.92; average total-pressure ratio, 0.99.

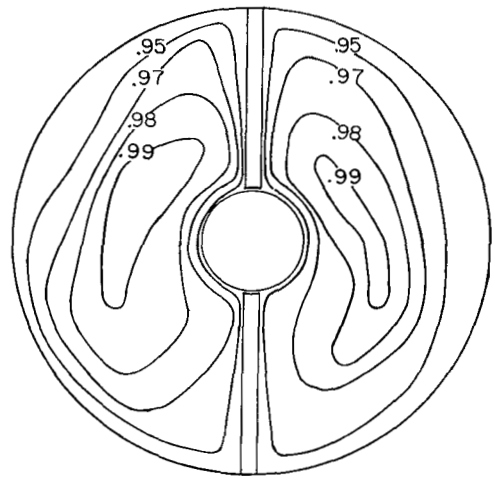

(b) $w/w_\infty = 0.52$; $\alpha = 10^\circ$; $\psi = 0^\circ$; average static-pressure ratio, 0.91; average total-pressure ratio, ~~0.98~~ .97

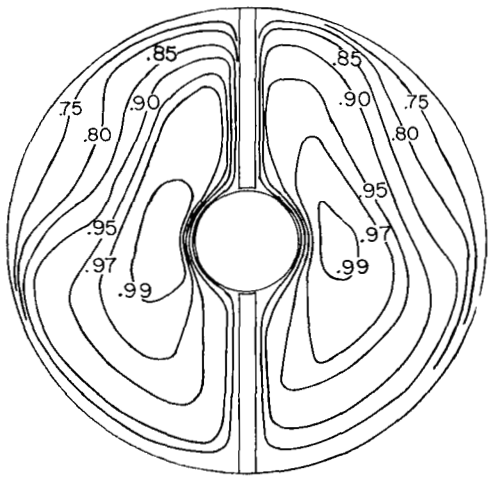

(c) $w/w_\infty = 0.89$; $\alpha = 0^\circ$; $\psi = 0^\circ$; average static-pressure ratio, 0.70; average total-pressure ratio, ~~0.95~~ .93

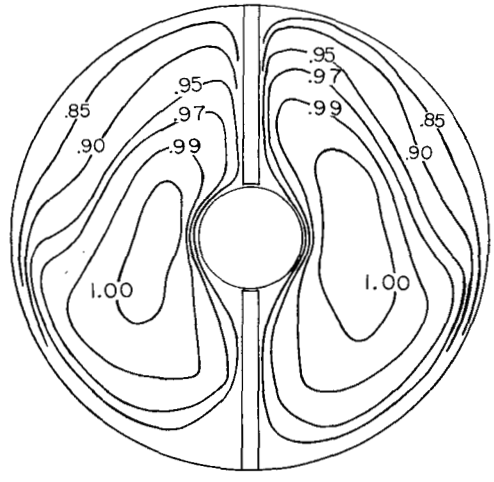

(d) $w/w_\infty = 0.84$; $\alpha = 0^\circ$; $\psi = -10^\circ$; average static-pressure ratio, 0.79; average total-pressure ratio, ~~0.98~~ .97

Figure 11.- Typical contour maps of total-pressure ratio at the compressor face at M = 0.90.

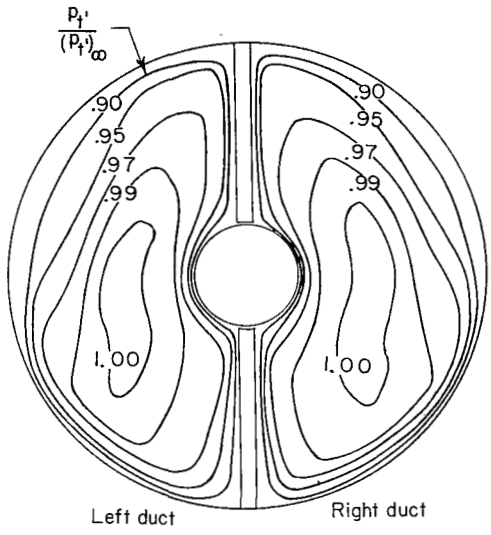

(a) $w/w_\infty = 0.70$; $\alpha = 0^\circ$; $\psi = 0^\circ$; average static-pressure ratio, 0.86; average total-pressure ratio, 0.98.

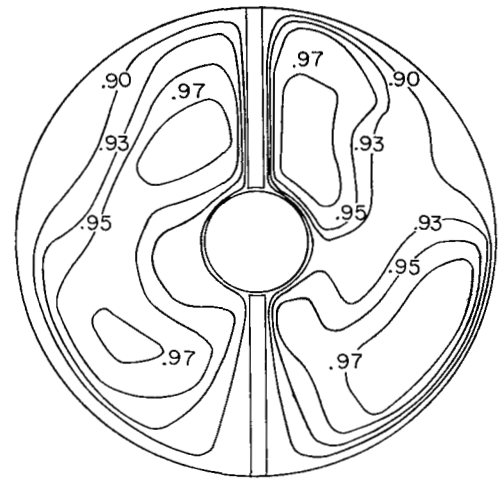

(b) $w/w_\infty = 0.69$; $\alpha = 10^\circ$; $\psi = 5.2^\circ$; average static-pressure ratio, 0.83; average total-pressure ratio, ~~0.96~~ .95.

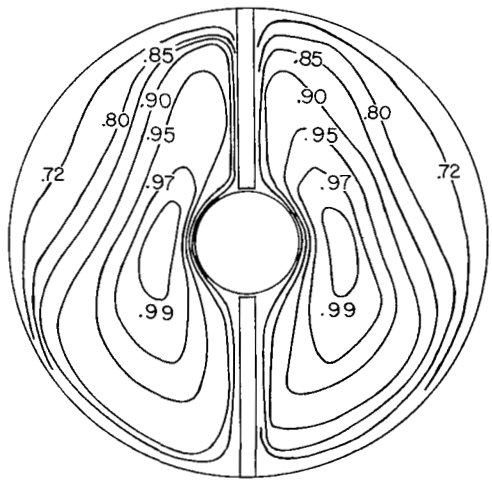

(c) $w/w_\infty = 0.87$; $\alpha = 0^\circ$; $\psi = 0^\circ$; average static-pressure ratio, 0.66; average total-pressure ratio, ~~0.93~~ .91.

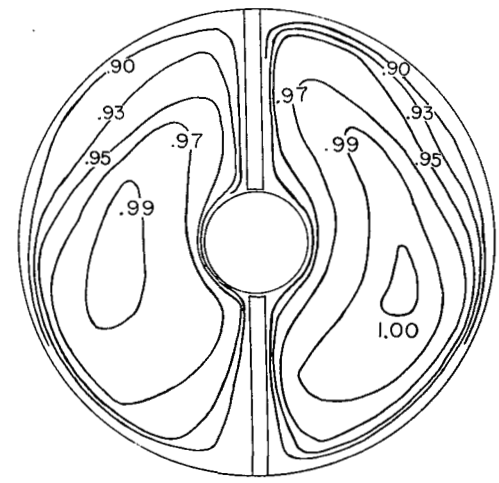

(d) $w/w_\infty = 0.70$; $\alpha = 0^\circ$; $\psi = -10^\circ$; average static-pressure ratio, 0.85; average total-pressure ratio, ~~0.98~~ .95; gloves on fuselage.

Figure 12.- Typical contour maps of total-pressure ratio at the compressor face at M = 1.10.